AFRL-AFOSR-VA-TR-2019-0181

Nanoantennas for Engineering Waves on the Surface (NEWS)

Hossein Mosallaei
NORTHEASTERN UNIVERSITY

11/28/2018
Final Report

Air Force Research Laboratory
AF Office Of Scientific Research (AFOSR)/ RTB1
Arlington, Virginia 22203
Air Force Materiel Command

REPORT DOCUMENTATION PAGE

Form Approved
OMB No. 0704-0188

1. REPORT DATE *(DD-MM-YYYY)*	**2. REPORT TYPE**	**3. DATES COVERED** *(From - To)*
11/06/2018	Final	09/30/2014-09/29/2018

4. TITLE AND SUBTITLE
Nanoantennas for Engineering Waves on the Surface

5a. CONTRACT NUMBER

5b. GRANT NUMBER
FA9550-14-1-0349

5c. PROGRAM ELEMENT NUMBER

6. AUTHOR(S)
Hossein Mosallaei

5d. PROJECT NUMBER

5e. TASK NUMBER

5f. WORK UNIT NUMBER

7. PERFORMING ORGANIZATION NAME(S) AND ADDRESS(ES)
Northeastern University
Office of Research Administration and Finance
960 Renaissance Park
360 Huntington Avenue

8. PERFORMING ORGANIZATION REPORT NUMBER

9. SPONSORING/MONITORING AGENCY NAME(S) AND ADDRESS(ES)
Air Force Office of Scientific Research

10. SPONSOR/MONITOR'S ACRONYM(S)
AFOSR

11. SPONSOR/MONITOR'S REPORT NUMBER(S)

12. DISTRIBUTION/AVAILABILITY STATEMENT
DISTRIBUTION A: DISTRIBUTION APPROVED FOR PUBLIC RELEASE

13. SUPPLEMENTARY NOTES

14. ABSTRACT

In this proposal, the PI will investigate metasurfaces nanoantennas to tailor unique photonic characteristics on surface. Nanoantennas will control amplitude, phase, and polarization. The objective is to make metasurfaces platforms for various disciplines including nanoscale, quantum, and bio-platforms. We will investigate fundamental science and engineer metasurfaces nanoantennas integrated in various areas including light processing, far and near fields manipulation, sensing and imaging, quantum-bio platforms, and electronically/dynamically controllable surfaces (and conformed to curved platforms).

15. SUBJECT TERMS

16. SECURITY CLASSIFICATION OF:			**17. LIMITATION OF ABSTRACT**	**18. NUMBER OF PAGES**	**19a. NAME OF RESPONSIBLE PERSON**
a. REPORT	**b. ABSTRACT**	**c. THIS PAGE**			**19b. TELEPHONE NUMBER** *(Include area code)*

To: technicalreports@afosr.af.mil
Subject: Annual Progress Statement to Dr. Gernot Pomrenke

Contract/Grant Title: Nanoantennas for Engineering Waves on the Surface
Contract/Grant #: FA9550-14-1-0349
Reporting Period: 30 September 2014 to 29 September 2018

Accomplishments: We have worked on various topics related to metasurfaces with 21 journal papers published [1-21]. The focus has been on metasurfaces with novel building blocks both plasmonic and all-dielectric, single and multilayer, and active. We have also implemented required modeling schemes. The topics can be summarized as, 1) all-dielectric metasurfaces, 2) plasmonic and all-dielectric nanoantennas building blocks, 3) multilayer configurations, 4) power limiter nonlinear metasurfaces, 5) ITO-based tunable metasurfaces, 6) tunable nanowires, 7) modeling and optimization.

1. All-Dielectric Metasurfaces, Flat and Conformal:

Here we have investigate the concept of all dielectric metasurfaces. We have considered disk building blocks where electric and magnetic modes are created and offer Huygens metasurface with full transmission and controllable phase. A metasurface lens is illustrated in transmission mode. The results are shown in Fig. 1 for bending performance. Full details can be found in [1].

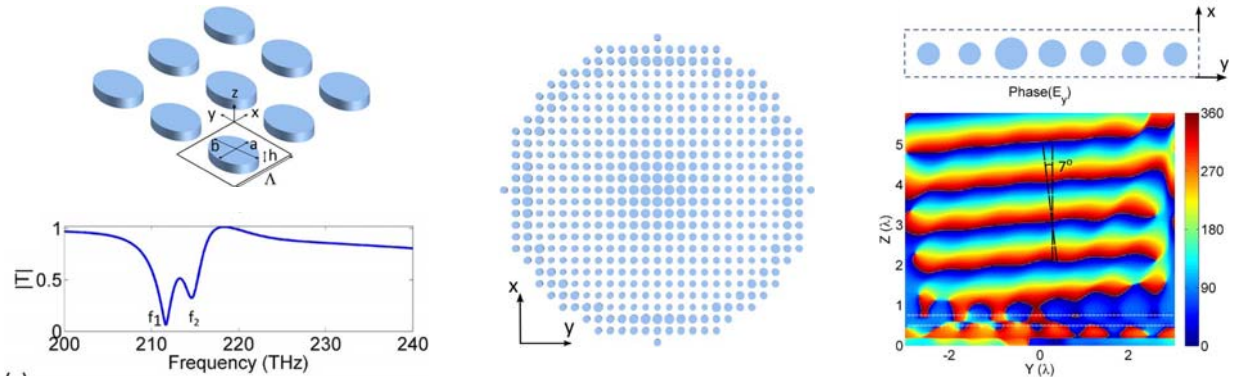

(a) (b) (c)

Figure 1. (a) Array of dielectric metasurface and its transmission performance, (b) an all-dielectric metasurface lens, and (c) bending performance and its full wave modeling.

We then took the concept to realize an achromatic design. Basically an issue with metasurfaces is their narrow bandwidth. We surpassed this by using a filter circuit theory idea when one can in theory overcome the issue. We designed layered metasurfaces each layer to provide requires LC element then by cascading to demonstrate a metasurface with wideband performance. We have enabled this both by using plasmonic elements and only-dielectric concept, illustrated in Fig. 2. Also Fig. 2 shows results for an all-dielectric design for focusing over the entire visible band. One can clearly see achromatic performance for focusing. Full details can be found in [2]. We have also extended the idea and realized by layered metasurfaces working based on effective material theory (and not resonant metasurfaces elements) where allowing to enhance even further the bandwidth, as shown in Fig. 3 [3].

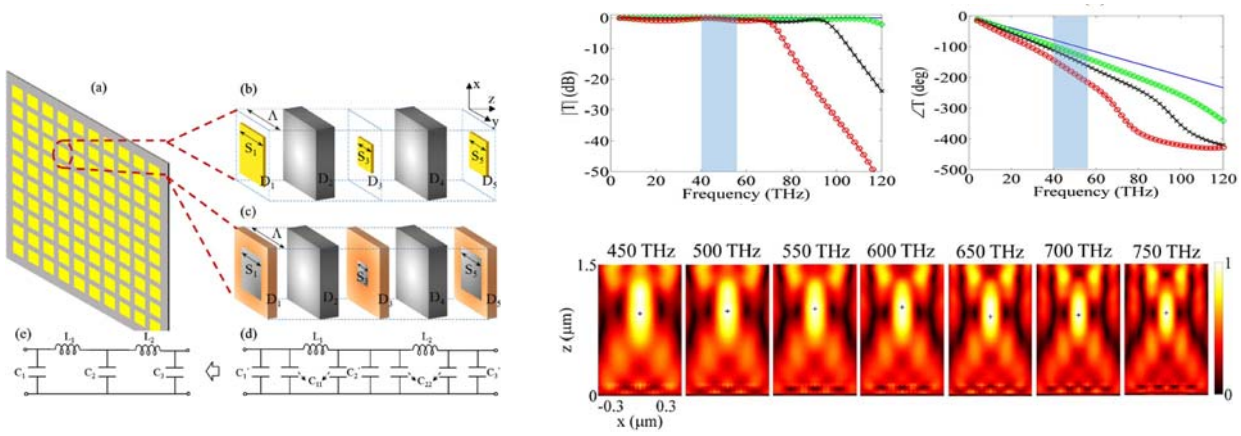

(a) (b)

Figure 2. (a) Layered dielectric metasurface realizing filter circuit theory, (b) transmission amplitude and linear phase performance, and (c) achromatic focusing over the visible band.

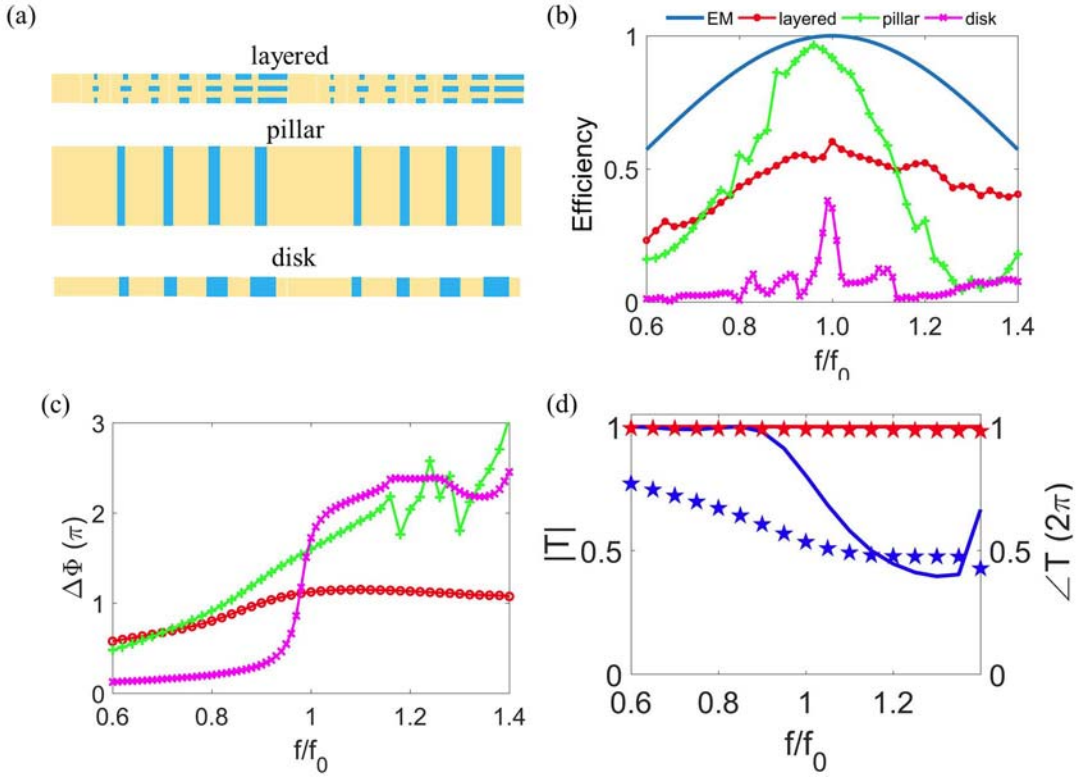

Figure 3. (a) Schematic illustration of the three metasurfaces by repeating two supercells in each. (b) Efficiency spectrum of the metasurfaces for 15 deg beam deflection. Solid line using effective material equation. Dot line, plus line and cross line are for layered, pillar and disk metasurfaces, respectively. (c) Variation of phase in the supcercell over frequency with the same legend as in (b). (d) Transmission amplitude and phase of the first (red) and the last elements (blue) in the layered supercell. Solid lines are amplitude and star markers are phase.

We also have worked on design and analyze conformal metasurfaces for practical optical applications at 532 nm visible band for the first time. The inclusions are silicon disk nanoantennas embedded in a flexible supporting layer of polydimethylsiloxane (PDMS). They behave as local phase controllers in subwavelength dimensions for successful modification of electromagnetic responses point by point, with merits of high efficiency, at visible regime, ultrathin films, good tolerance to the incidence angle and the grid stretching due to the curvy substrate. An efficient modeling technique based on field equivalence principle is systematically proposed for characterizing metasurfaces with huge arrays of nanoantennas oriented in a conformal manner. Utilizing the robust nanoantenna inclusions and benefiting from the powerful analyzing tool, we successfully demonstrate the superior performances of the conformal metasurfaces in two specific areas, with one for lensing and compensation of spherical aberration, and the other carpet cloak, both at 532 nm visible spectrum. We have implemented conformal metasurfaces for cloaking and lensing applications using all dielectric elements at 532 nm. ([4])

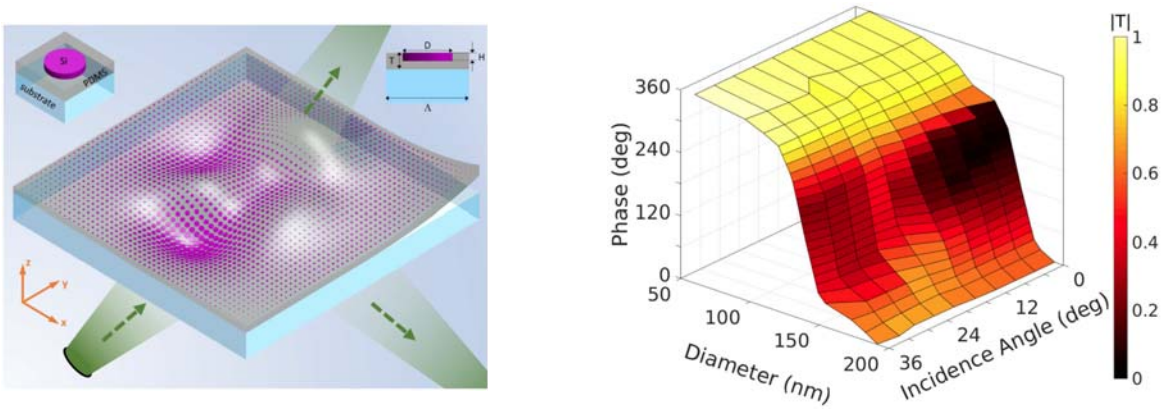

(a) (b)

Figure 4. (a) Schematic of a conformal metasurface wrapping onto an arbitrarily curved platform, (b) Transmission responses of dielectric disk elements with variation of diameters and oblique incident angle.

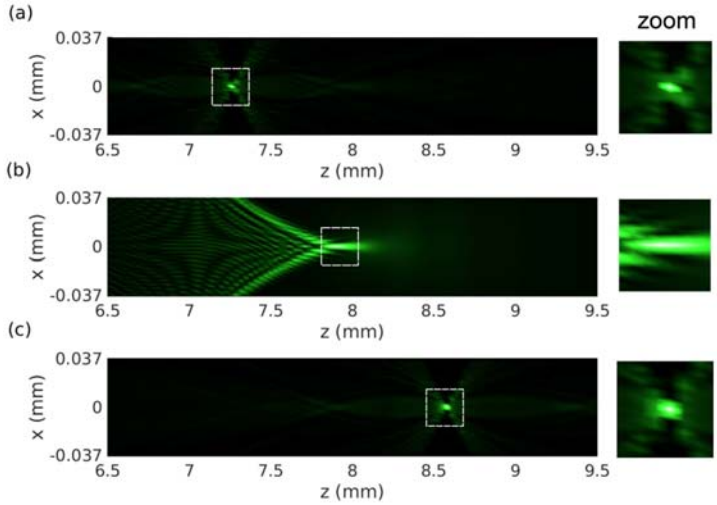

Figure 5. The focal length is modified into 7.2 mm in (**a**) and 8.5 mm in (**c**) with minimized spherical aberration by coating two types of metasurface layers with proper disk diameter profiles, compared to the performance of the original lens in (**b**). The field within the dashed square is zoomed in on the right for each case.

2. Nanoantennas Building Blocks, Plasmonic and All-Dielectric:

Our group has worked extensively as part of this program to study various nanoantennas building blocks for metasurfaces, both plasmonic and all-dielectric. Figure 6 illustrates a double concentric loops. Proper design and coupling between the loops allow for full transmission and phase control as is desired. Another unique feature of this design is that for a desired phase change we have to rotate the element by double the angle. No need to stress that it also works in transmission mode (in contrast to many metasurface in reflection mode). We have taken the idea to implement a metasurface for beam shaping as is shown in Fig. 6 (c). The metasurface actually does two things, 1) control the ray path to change a Gaussian beam to a flat top beam, and 2) to conjugate phase and allow uniform phase after transmission for long propagation length. Full study in [5].

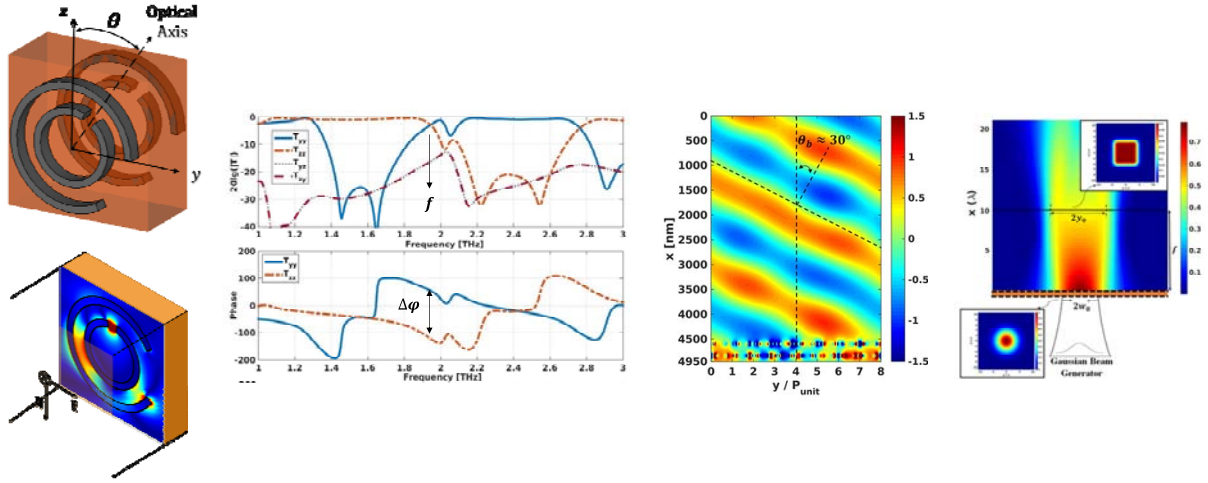

(a) (b) (c)

Figure 6. (a) Double concentric plasmonic loop for full transmission and phase control and its amplitude and phase performance, (b) bending, and (C) beam shaping performance.

A systematic study is also carried out on the interaction of electromagnetic waves with a nonsymmetric all-dielectric C-shaped nanoantenna to achieve an ultimate control over the independent and relative spectral positions of the excited magnetic and electric dipolar modes. By properly determining the structural parameters (inner and outer radii and the opening angle) and tailoring the interference of geometrical resonances, an ultrathin C-element metasurface is designed, which can highly transmit the linearly polarized incident beam (>80%) with full phase-agility (2π) in the red light of visible regime. The investigation on the physical mechanism behind this nanoantenna reveals the confinement of magnetic and electric fields corresponding to the magnetic and electric dipolar modes mainly inside the hollow and opening angle, i.e., outside the constituent high-index material of C-element. This feature allows making building blocks less dependent on the material loss and dispersion. Three different approaches based on only varying the inner/outer radius or the opening angle are proposed which can facilitate the design complexity, the encoding of the desired phase distribution for specific functionality, and easing the fabrication procedure. The proposed approaches are leveraged to design several highly transparent graded-pattern metasurfaces with the capability of beam steering, focusing, flat-top generation, and holography [6]. Figures 7 and 8 show the concept and results.

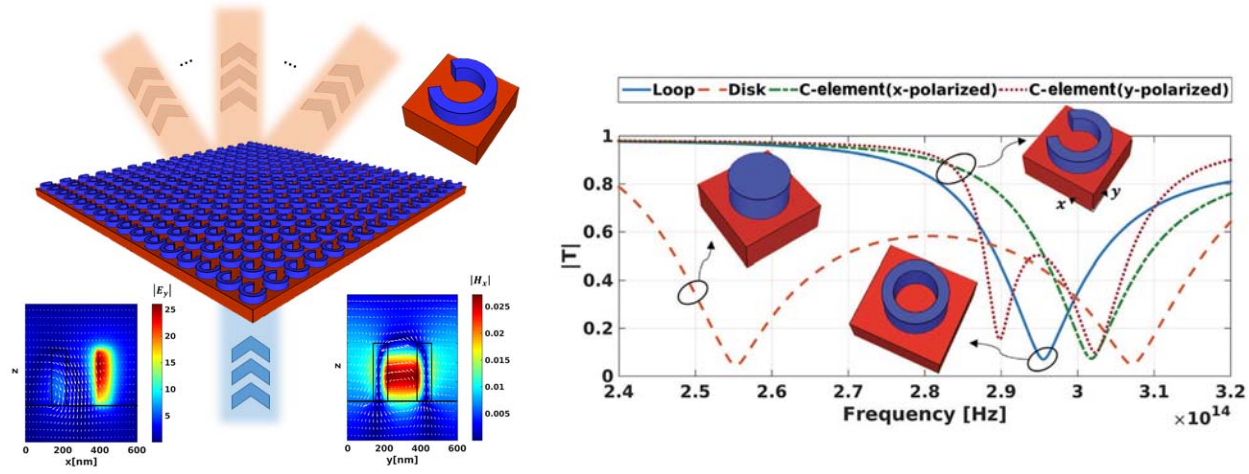

(a) (b)

Figure 7. (a) Schematic representation of the proposed all-dielectric metasurface for beam manipulation, (b) The transmission amplitude of the periodic C-shaped unit-cell for x-polarized (dash-dotted line) and y-polarized (dotted line) incident beams. The dashed and solid lines are related to the transmission responses of two limiting cases when $R_i = 0$ and $\alpha = 0$ (nanodisk) and $R_i \neq 0$ and $\alpha = 0$ (nanoloop), respectively. The insets show the prospective views of corresponding unit-cells.

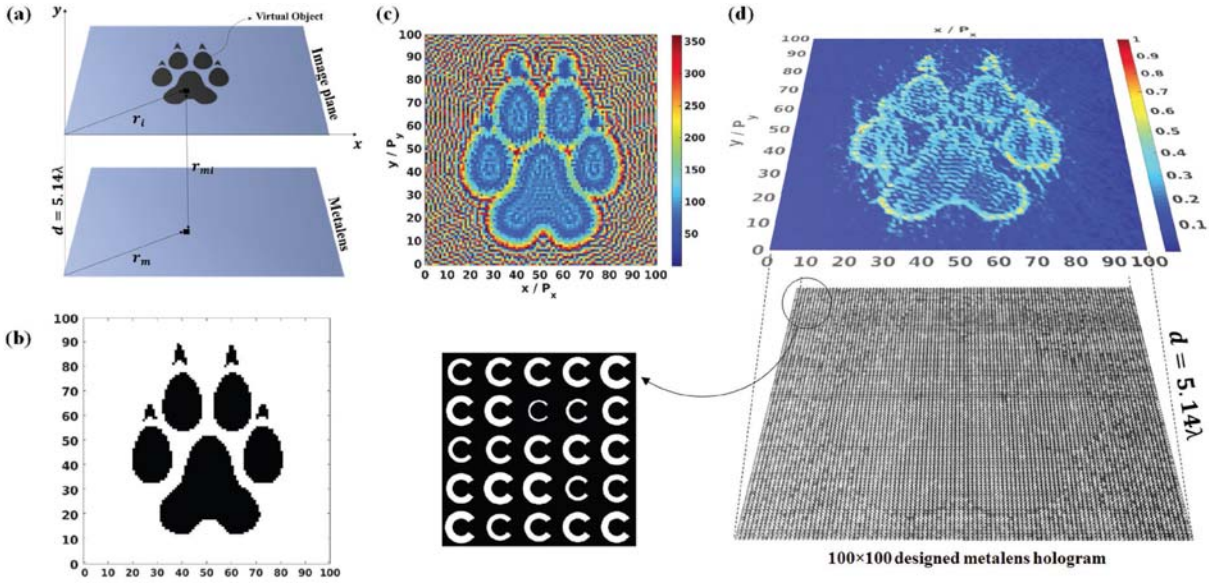

Figure 8. (a) Schematic illustration of the metasurface hologram design. The image plane is assumed at the distance of $d = 5.14\lambda$ above the metasurface hologram where the light-emitting virtual object ("husky logo") is located. The required electric field distribution on the metalens is calculated based on the diffraction theory and mapping the electric field propagating from the virtual object. (b) The binary image of the "husky logo" which includes 100×100 pixels. The black region has the same amplitude of 1 and the white region around the object has the amplitude of 0. (c) The calculated phase distribution of the electric field on the metasurface plane. (d) The numerically calculated amplitude of the electric field distribution at the image plane ($d = 5.14\lambda$) at the operating frequency of 430 THz. The holographic image is produced by 100×100 array of C-elements with only varying outer radius (this is a very huge array size we have modeled).

3. Composite Multilayer Metasurfaces:

A dual-band multilayer shared aperture antenna (SAA) is presented, which can recognize anomalous two-dimensional beam steering simultaneously at two distinct operating wavelengths lie in near-infrared (NIR) (1055 nm) and visible (700 nm) spectra. The supercell consists of one large cross-shaped resonator antenna (top layer) and a 2 × 2 square-shaped patches (bottom layer). This compact bifunctional dual-band reflectarray SAA can steer the main beam toward relatively large angles (≈40 deg) in both θ- and φ-planes at dual-frequency bands. The state-of-the-art techniques in antenna design are exploited to attain the minimized aperture size and negligible coupling among NIR and visible arrays. The overall height of the antenna is 275 nm. The presented structure is customizable in form and can easily be scaled to other frequency ratios. ([7])

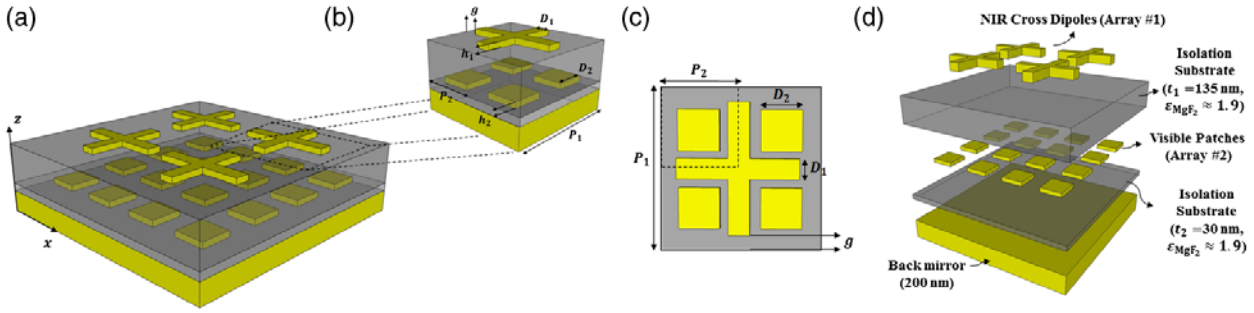

Figure 9. (a) Schematic of dual-band multilayer shared aperture reflectarray antenna, (b) three dimensional and (c) top view of the proposed supercell, and (d) illustration of the topological orientation of the SAA.

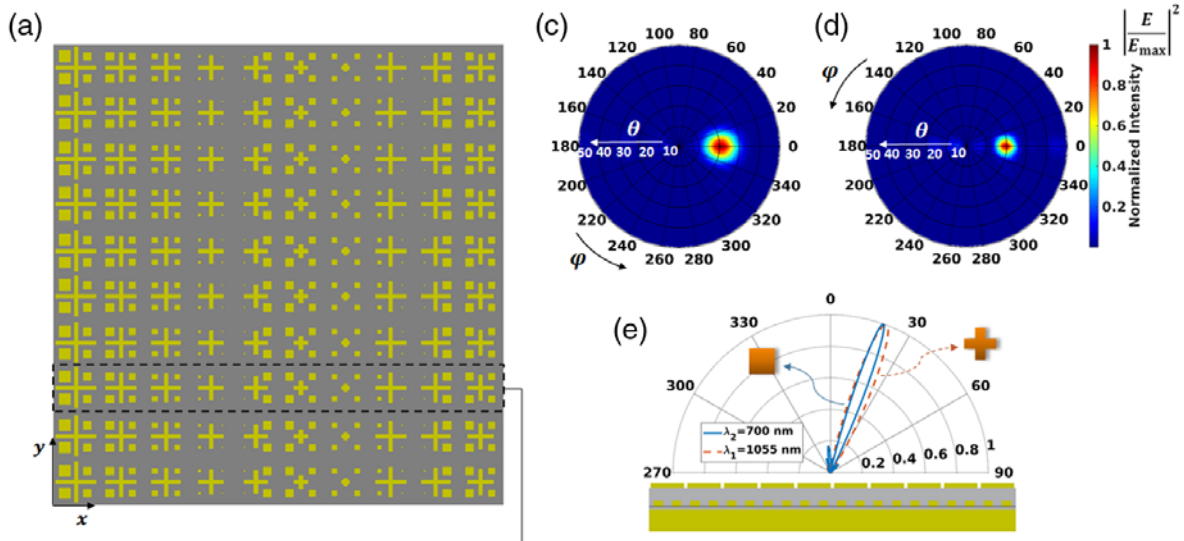

Cross Dipoles (deg)									
0	58	117	175	234	292	351	49	108	166
Square Patches (deg)									
0	44	88	132	176	221	265	309	353	37
81	125	169	214	258	302	346	30	74	118

Figure 10. (a) Schematic of the designed SAA, (b) the required phase delay to achieve simultaneous similar beam steering toward [θ, φ]=[20°, 0°]. (c)-(d) 2D normalized intensity of the reflected beam at 1055 nm and 700 nm. (e) The results in (c)-(d) in the x-z plane.

We have also extended the concept and for more general platforms of dielectric and TCO materials as illustrated in Fig. 11 [8]. We have investigated fully the concept taking the coupling between the layers and using materials parameters. Figure 11 shows light manipulation via the dual-wavelength out-of-plane holographic metalens for reconstructing two holographic images at two separate planes of 10λ1 and 2λ2 away from the metalens. The image planes are chosen at the distances of 10λ1 and 2λ2 above the shared aperture metasurface hologram where the virtual objects of a "leaf" and a "flame" are placed, respectively. Numerically calculated amplitude of the electric field distributions at the image planes (10λ1 and 2λ2) at the operating frequencies of 531 and 37 THz under illumination of circularly and linearly polarized incident beams, respectively.

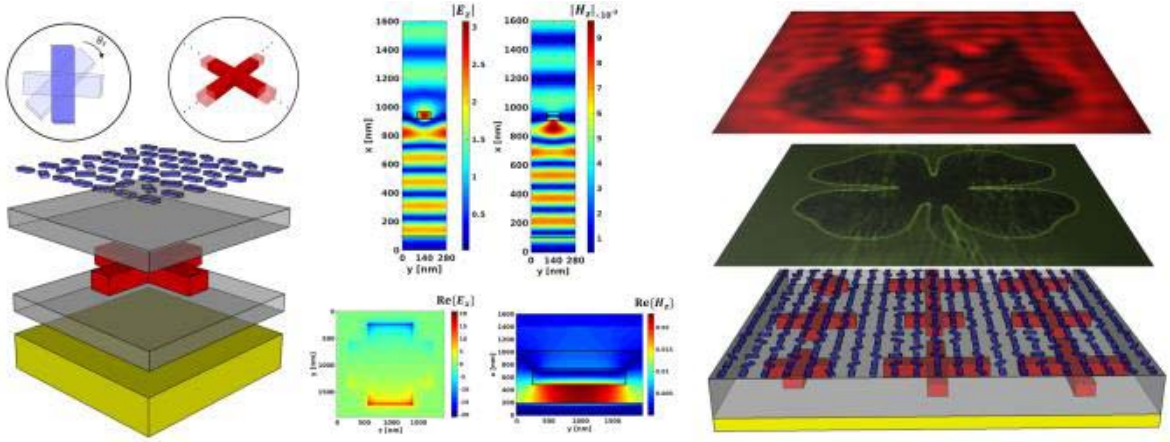

Figure 11. Schematic demonstration of the topological orientation of the dual-band multilayer TCO−dielectric shared-aperture antenna. Also the numerical results for operation at two bands, IR and visible.

4. Laser Power Limiter Metasurface (including nonlinear material):

A novel low-profile nonlinear metasurface, consisting of a single-layer of all-dielectric material, is proposed and numerically investigated by a nonlinear full-wave finite difference time-domain (FDTD) method. The proposed metasurface is transparent for low, and opaque for high values of incident light intensity. The metasurface design is broadly applicable to enhancement of intrinsic nonlinearities of any material with a sufficiently high refractive index contrast. We illustrate the ability of this design to enhance intrinsic nonlinear absorption of a transition metal oxide, vanadium pentoxide (V2O5), with resonant metasurface elements. The complex third-order nonlinear susceptibility for V2O5, representing both nonlinear refraction and absorption is considered in FDTD simulations. Our design achieves high initial transparency (>90%) for low incident light intensity. An order of magnitude decrease in the required input light intensity threshold for nonlinear response of the metasurface is observed in comparison with an unpatterend film. The proposed all-dielectric metasurface in this work is ultrathin and easy to fabricate. We envision a number of applications of this design for thin film coatings that offer protection against high-power laser radiation. ([9])

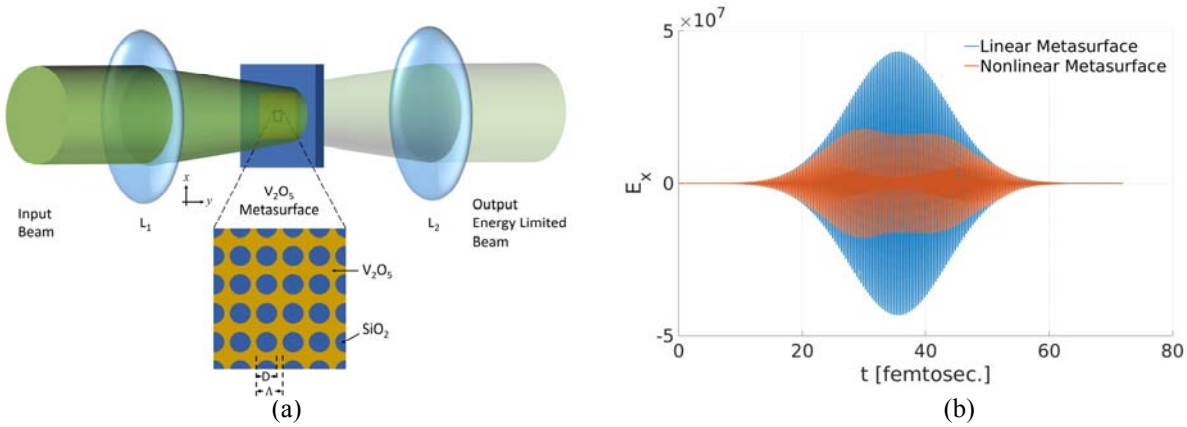

Figure 12. (a) A representative schematic of the proposed nonlinear optical metasurface consisting of a periodic array of air holes in a V2O5 layer, deposited on a silica substrate, (b) Transient response of the V2O5 metasurface to a modulated Gaussian incident waveform in the far-field region. The peak intensity of the input signal is 109 W/cm2. The response of the linear metasurface with the same refractive index as V2O5 is also plotted for reference.

5. Tunable Metasurfaces by ITO:

We have worked extensively on tunable metasurfaces using ITO materials. This is to have controllable behavior in real-time by applying voltages to ITO [10-12]. One of our works in this area has been 2016 highlight in Journal of Optics [12].

In our work [10] we design two electrically tunable dual-band reflectarray antennas by the integration of a thin layer of indium tin oxide (ITO) into plasmonic multi-sized and multilayer unit cells. The presented geometries include two gold nanoribbons located next to each other with different widths and backed by a stack of alumina-ITO-metallic ground plane and two pairs of vertically stacked gold nanoribbon-alumina-ITO on a metallic ground plane. The double-resonance nature of the double metal-insulator metal unit-cells is exploited to achieve two distinct operating frequencies in which the control over phase of the reflected beam is obtained via the tunable gate biasing of ITO. An in-depth phased array analysis is developed with emphasis on the accomplishment of a reconfigurable antenna with robust beam scanning and focusing characteristics. The proposed structures can be considered as dual-band bifunctional reflectarray antenna that can operate at two distinct frequencies in the near-infrared regime with two different functionalities as bending and focusing. In [12] we extend to 2D beam scanning.

We have recently extended this concept using all dielectric metasurfaces [13]. Basically we design Si disks to be coupled to ITO layers and to be tuned successfully. Full study is in progress. We have also enabled tunable metasurfaces using graphene sheets [14].

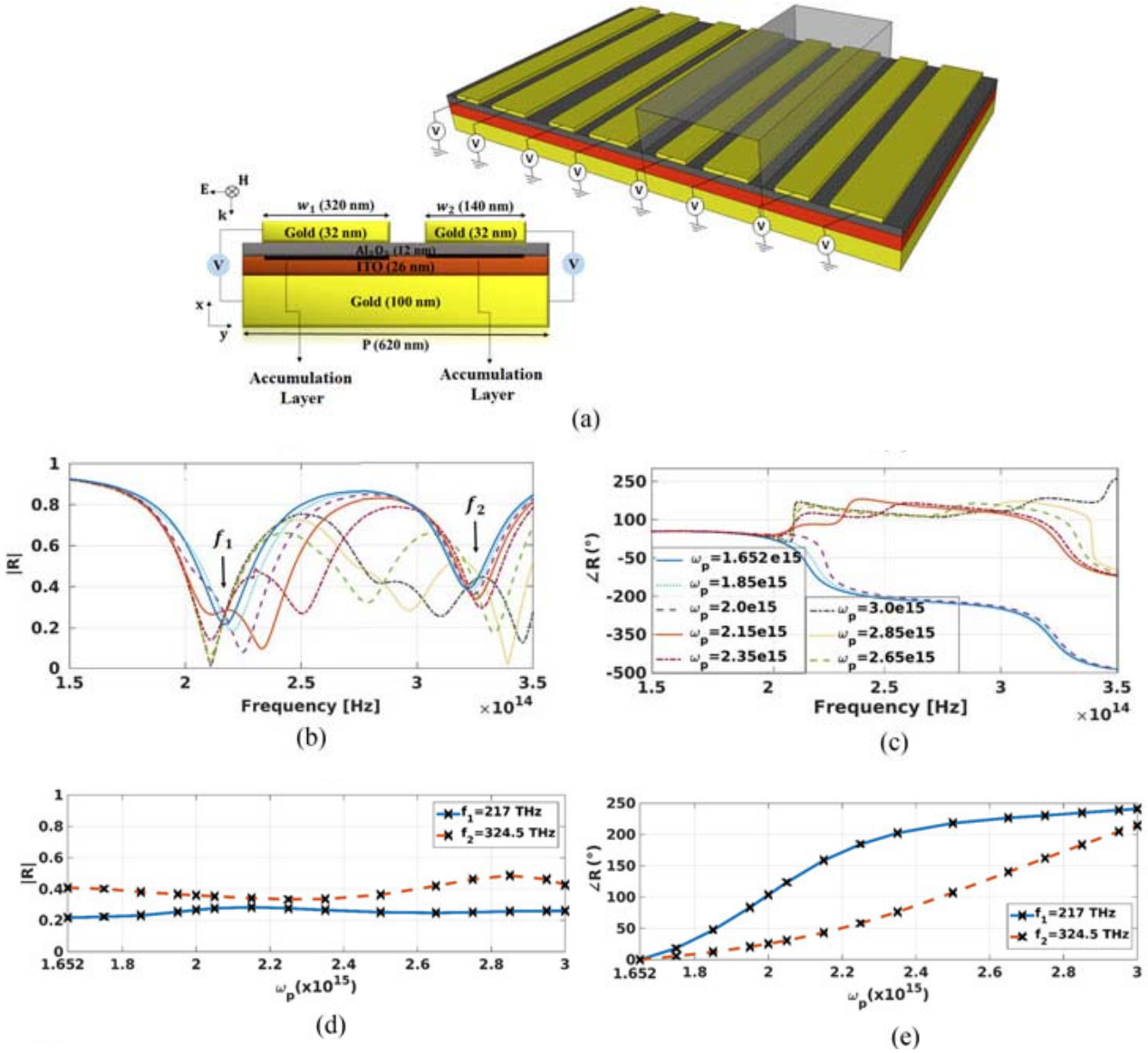

Figure 13. (a) Schematic overview of the electrically tunable dual-band reflectarray structure. The bi-MIM unit-cell includes two nanoribbons which are placed on a stack of Al_2O_3-ITO-gold back mirror. FDTD full-wave simulation results for the reflection (b) amplitude and (c) phase of the unit-cell versus frequency for different plasma frequencies of the accumulation layers of ITO in the range from 1.652×10^{15} to 3×10^{15} rad/s. (d)-(e) The reflection amplitude and relative phase change (the reflection phase of the unbiased case is assumed zero) at the operating frequencies of 217 and 324.5 THz. Both gold nanoribbons are assumed under influence of the same DC voltage bias.

6. Electronically Tunable Nanowires:

We integrate indiumtin-oxide (ITO) as a tunable electro-optical material into multimaterial nanowires with metal-oxide semiconductor and metal-insulator-metal configurations. In particular, an active metasurface operating in the transmission mode is designed which allows for modulation of the transmitted light phase over 280 degrees. We demonstrate the use of such active metasurfaces for tunable bending and focusing in free-space. In the theoretical modeling, we adopt a hierarchical multiscale

approach by linking drift-diffusion transport model with the electromagnetic model which rigorously characterizes the electro-optical effects. ([15])

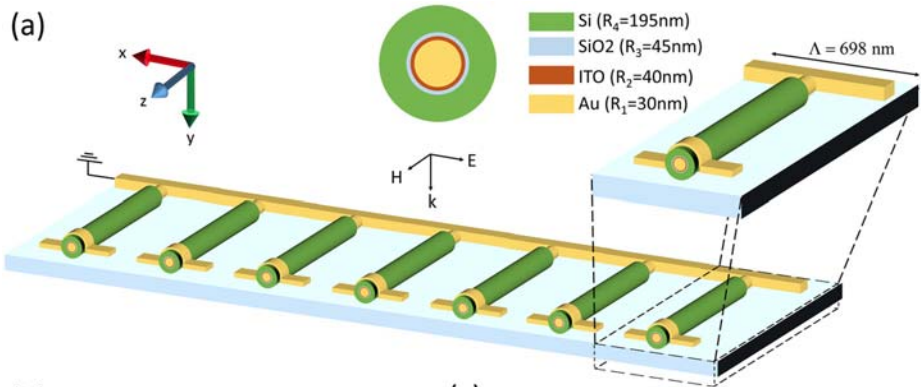

Figure 14. The schematic and geometrical parameters of the tunable metasurface operating in the transmission mode utilizing multimaterial nanowires.

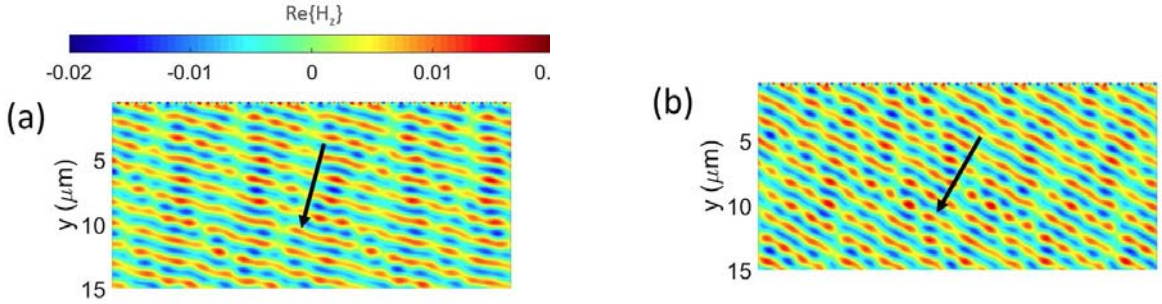

Figure 15. Tunable beam steering. The plane wave is incident normally to the metasurface and is traveling along y axis. Electronic Beam tuning by applying voltages to multimaterial nanowires. ((a) for 15^0 and (b) for 30^0)

We have also combined the designed nanowires with layered substrate and tunable to have a mechanism for tunable performance in far infrared (graphene based), IR (ITO), and visible (mechanical actuation). Full theoretical modeling is proposed to comprehensively study the performance [16]. We have also demonstrated a first tunable magnetization in IR by embedding nanowires in ENZ materials and tune the performance accordingly [17].

7. Modeling and Optimization:

Given the complexity and large area metasurfaces we deal with, powerful and fast computational models are essential. We have implemented methods based on DDA and integral equations for successful simulations. Also we have implemented optimization technique to optimize unique designs.

7. 1. DDA Technique: Advances in the field of metasurfaces require simulation of large-scale metasurfaces that extend over many light wavelengths. Adopting standard numerical methods leads to models featuring a large number of degrees of freedom, which are prohibitive to solve within a time window compatible with the design workflow. Therefore, this demands developing the techniques to replace large-scale computational models with simpler ones, still capable of capturing the essential features but imposing a

fraction of the initial computational costs. In this work, we present a simulation approach in order to handle reduced order analyses of large-scale metasurfaces of arbitrary elements. We use the discrete dipole approximation in conjunction with the discrete complex image method and hierarchical matrix construction as a common theoretical framework for dipole approximation in the hierarchy of individual elements and the array scale. We extract the contributions of multipoles in the scattering spectra of the nanoantennas forming the metasurface and retrieve their dynamic polarizabilities. The computational complexity of modeling the array problem is then significantly reduced by replacing the fine meshing of each nanoantenna with its dynamic polarizability. The solver is developed to model several fully functional metasurfaces of different types including a one-atom-thick metasurface made of graphene with chemical doping interruptions, a multi-focusing lens made of plasmonic V-shaped nanoantennas, and a multicolor hologram consisting of dielectric nanobars. The performance of the method is evaluated through comparison with full-wave simulations, and a significant computational gain is observed while the accuracy of the results is retained owing to the preserved coupling information between dipolar modes. (([18])

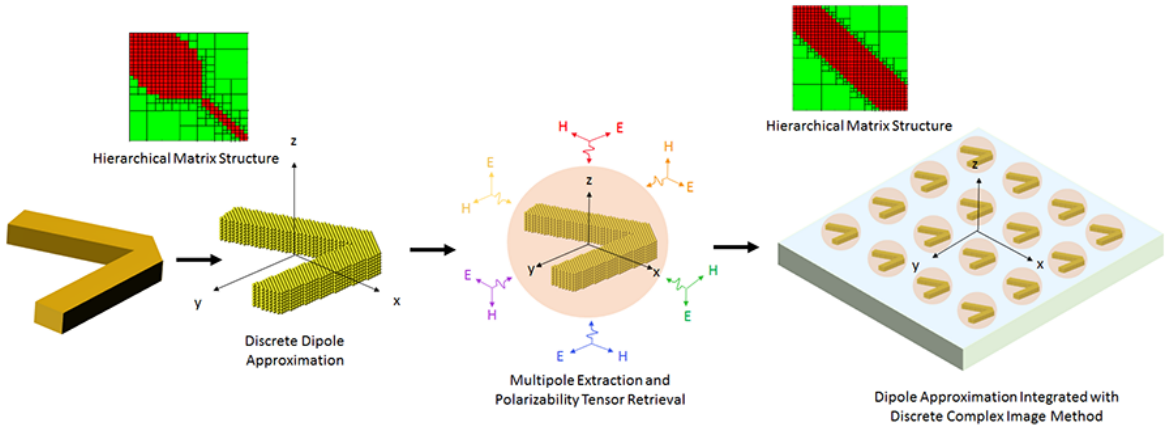

Figure 16. Schematic of the hierarchical multiscale DDA modeling

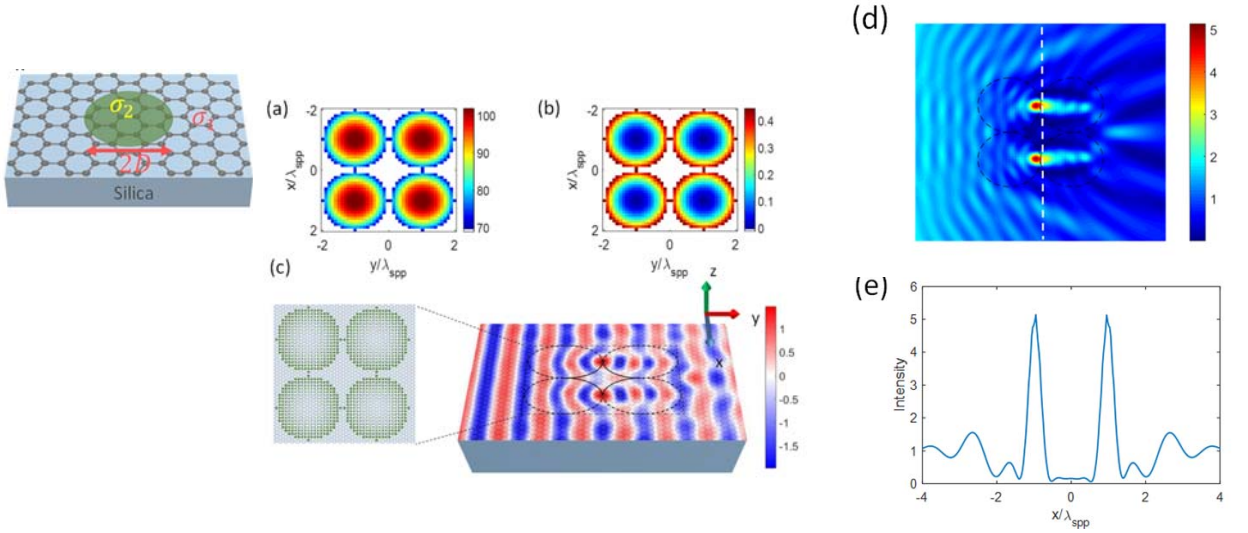

Figure 17. (a) Distribution of the effective refractive index and (b) the corresponding filling factor of the metasurface unit cells of graphene disks. (c) real part and (d) intensity of the field in y-x plane. The geometry of graded chemical interruptions in each Luneburg lens is illustrated in the inset of (c). (e) The intensity distribution along white dashed line in (d).

7. 2. Integral Equations:

We implement integral equation (IE)-based computational model for electromagnetic (EM) characterization of freestanding and substrate-supported 2D sheet structures. The freestanding 2D sheet is modeled with surface integral equation (SIE) method by combing the impedance boundary condition (IBC), while regarding the thickness of 2D sheet as zero. For the substratesupported 2D sheet structure, we start from the coupled volume and surface integral equations (VSIE) based on the field equivalence principle. Because of the infinitesimal thickness of 2D sheets and the introduction of the equivalent surface currents on the sheet, the volume integral has been successfully transformed to a surface integral, which avoids the computationally expensive volume discritization for 2D sheet structures. An efficient surface integral equation model is proposed. The domain decomposition method (DDM) is also employed, which decomposes the original large problem into smaller discrete sub-domain problems and brings the reduction both in computational time and memory [19].

Integral Equations Formulation:

$$\textbf{JMCFIE}\quad \begin{matrix}\mathrm{EFIE}_i+\eta_i\hat{n}_{ij}\times\mathrm{MFIE}_i+\mathrm{EFIE}_j+\eta_j\hat{n}_{ji}\times\mathrm{MFIE}_j\\ \hat{n}_{ij}\times\mathrm{EFIE}_i+\eta_i\mathrm{MFIE}_i+\hat{n}_{ji}\times\mathrm{EFIE}_j+\eta_j\mathrm{MFIE}_j\end{matrix}$$

$$\mathrm{EFIE}_i\quad \sum_{k\in C_i}\left(\eta_i L_i(\mathbf{J}_{ik})-K_i(\mathbf{M}_{ik})\right)_{\tan}+\frac{1}{2}\hat{n}_{ij}\times\mathbf{M}_{ij}(\mathbf{r})=\left(\mathbf{E}_i^{\mathrm{inc}}(\mathbf{r})\right)_{\tan},\ \mathbf{r}\in S_{ij}$$

$$\mathrm{MFIE}_i\quad \sum_{k\in C_i}\left(K_i(\mathbf{J}_{ik})+\frac{1}{\eta_i}L_i(\mathbf{M}_{ik})\right)_{\tan}-\frac{1}{2}\hat{n}_{ij}\times\mathbf{J}_{ij}(\mathbf{r})=\left(\mathbf{H}_i^{\mathrm{inc}}(\mathbf{r})\right)_{\tan},\ \mathbf{r}\in S_{ij}$$

$$L_i(\mathbf{X}_i)=jk_i\int_S\mathbf{X}_i(\mathbf{r}')G_i(\mathbf{r},\mathbf{r}')dS'-\frac{1}{jk_i}\nabla\int_S\nabla'\cdot\mathbf{X}_i(\mathbf{r}')G_i(\mathbf{r},\mathbf{r}')dS'\qquad K_i(\mathbf{X}_i)=PV\int_S\mathbf{X}_i(\mathbf{r}')\times\nabla G_i(\mathbf{r},\mathbf{r}')dS'$$

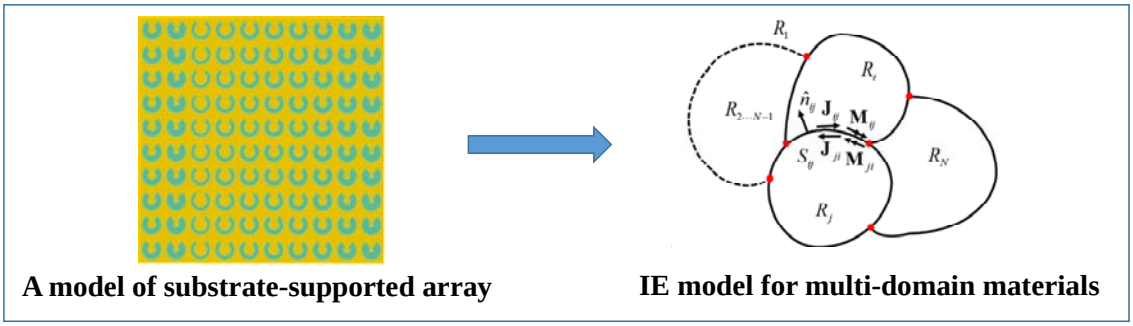

Figure 18. Schematic of the domain decomposition method (DDM) to break the computational domain into smaller regions, allowing fast computation of large array platforms/

7.3. Optimization Based Metasurfaces: Synthesization of multiple functionalities over a flat metasurface platform offers a promising approach to achieving integrated photonic devices with minimized footprint. Metasurfaces capable of diverse wavefront shaping according to wavelengths and polarizations have been demonstrated. Here we propose a class of angle-selective metasurfaces, over which beams are reflected following different and independent phase gradients in the light of the beam direction. Such powerful feature is achieved by leveraging the local phase modulation and the non-local lattice diffraction via inverse scattered field and geometry optimization in a monolayer dielectric grating, whereas most of the previous designs utilize the local phase modulation only and operate optimally for a specific angle. Beam combiner/splitter and independent multibeam deflections with up to 4 incident angles are numerically demonstrated respectively at the wavelength of 700 nm. The deflection efficiency is around 45% due to the material loss and the compromise of multi-angle responses. Flexibility of the approach is further validated by additional designs of angle-switchable metagratings as splitter/reflector and transparent/opaque mirror. The proposed designs hold great potential for increasing information density of compact optical components from the degree of freedom of angle. ([20])

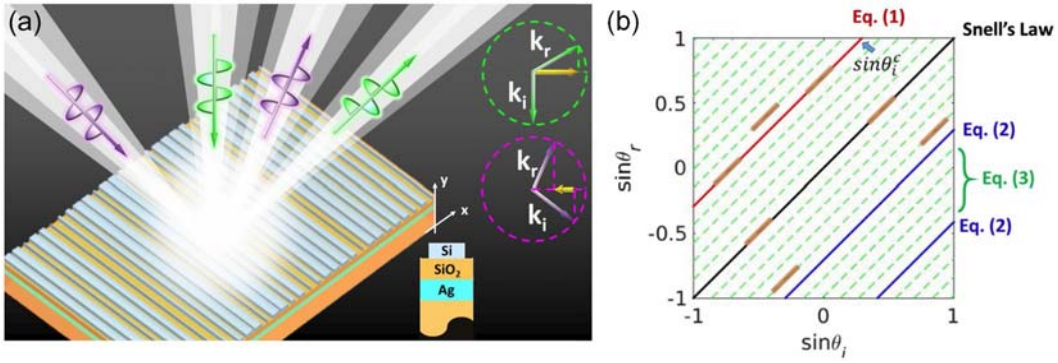

Figure 19. (**a**) Optimized metagrating for angle-selective beam deflection. Different phase gradients can be seen by beams from different directions, leading to independent beam deflections controlled by angle. The momentum conservation is illustrated in the upper right corner, with the metasurface phase gradient represented by the yellow arrow. The reflective grating element is shown in the lower right corner. (**b**) Snell's law of reflection and its generalization.

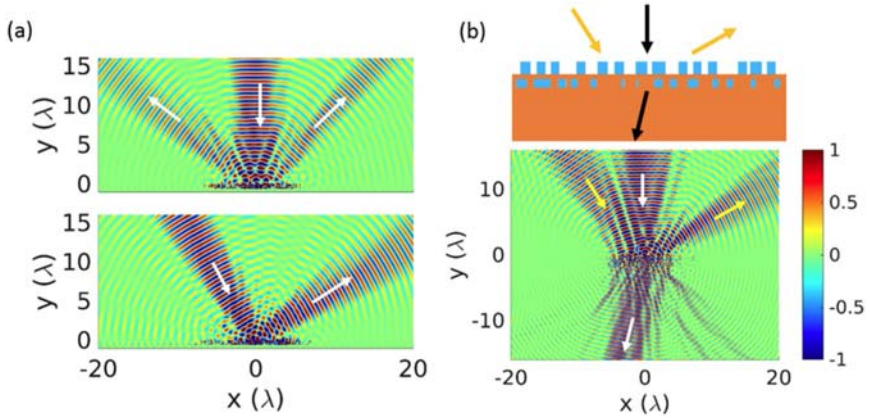

Figure 20. (**a**) Metagrating as beam splitter and reflective mirror with the function switchable by the incident angle. (**b**) Bi-layer metagrating optimized for selective transmission and reflection. The lattice supercell is shown on top of the field plot. The top and bottom bar layers are separated by 200 nm spacer with the bar thickness of 600 nm and 400 nm, respectively.

7.4. Genetic Algorithm Based Design: As optical metasurfaces become progressively ubiquitous, the expectations from them are becoming increasingly complex. The limited number of structural parameters in the conventional metasurface building blocks, and existing phase engineering rules do not completely support the growth rate of metasurface applications. We present digitized-binary elements, as alternative highdimensional building blocks, to accommodate the needs of complex-tailorable-multifunctional applications. To design these complicated platforms, we demonstrate adaptive genetic algorithm (AGA), as a powerful evolutionary optimizer, capable of handling such demanding design expectations. We solve four complex problems of high current interest to the optics community, namely, a binarypattern plasmonic reflectarray with high tolerance to fabrication imperfections and high reflection efficiency for beam-steering purposes, a dual-beam aperiodic leaky-wave antenna, which diffracts TE and TM excitation waveguides modes to arbitrarily chosen directions, a compact birefringent alldielectric metasurface with finer pixel resolution compared to canonical nano-antennas, and a visibletransparent infrared emitting/absorbing metasurface that shows high promise for solar-cell cooling applications, to showcase the advantages of the combination of binary-pattern metasurfaces and the AGA technique. Each of these novel applications encounters computational and fabrication challenges under conventional design methods, and is chosen carefully to highlight one of the unique advantages of the AGA technique. We show that large surplus datasets produced as by-products of the evolutionary optimizers can be employed as ingredients of the new-age computational algorithms, such as, machine learning and deep leaning. In doing so, we open a new gateway of predicting the solution to a problem in the fastest possible way based on statistical analysis of the datasets rather than researching the whole solution space. Full details can be found in [21].

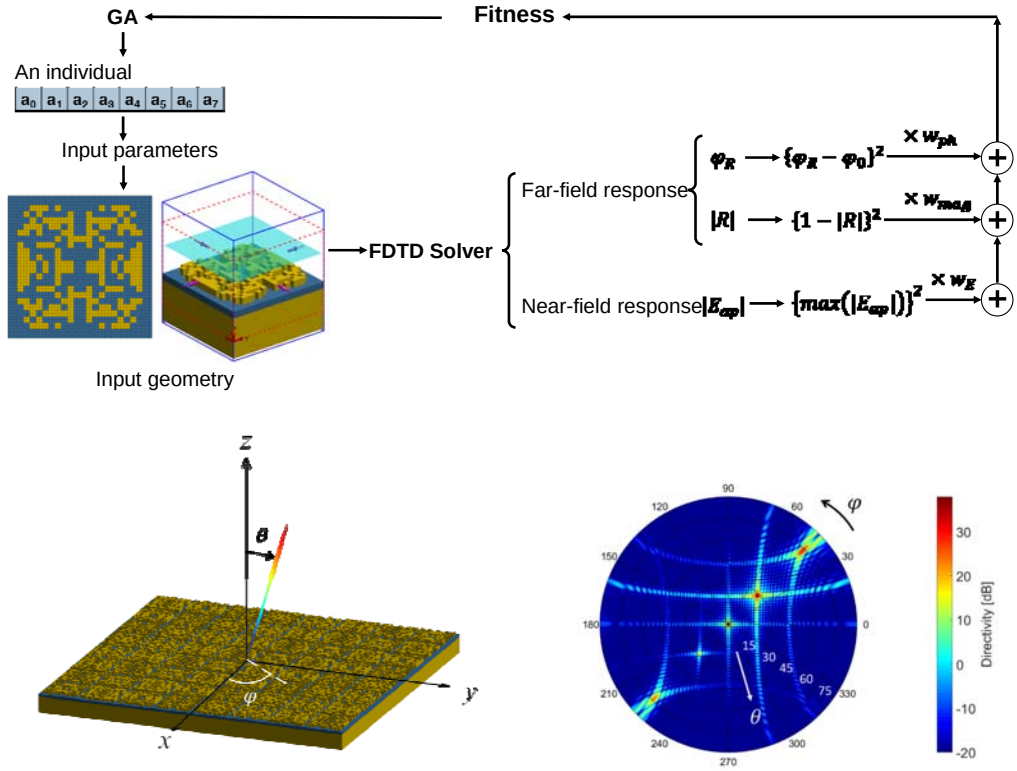

Figure 21. GA optimized metasurface and associated cost function, designed metasurface, and the beam scanning in space managed by the optimized metasurface.

Archival Publications:

1. J. Cheng, D. Ansari, and H. Mosallaei, "Wave manipulation with designer dielectric metasurfaces," *Optics Lett,* vol. 39, no. 21, Nov. 2014.
2. J. Cheng and H. Mosallaei, "Truly achromatic optical metasurfaces: A filter circuit theory based-design," *JOSA B,* vol. 32, no. 10, pp. 2115-2121 (2015).
3. J. Cheng, S. Inampudi, F. Fan, X. Wang, S. Chang, and H. Mosallaei, "Dielectric metasurfaces in transmission and reflection modes approaching and beyond bandwidth of conventional blazed grating," *Optics Express,* Vol. 26, No. 10, May 2018.
4. J. Cheng, S. Jafar-Zanjani, H. Mosallaei, "All-dielectric ultrathin conformal metasurfaces: lensing and cloaking applications at 532 nm wavelength," *Scientific Report,* 6, 38440, DOI: 10.1038/srep38440, 2016.
5. A. Forouzmand, S. Tao, S. Jafar-Zanjani, J. Cheng, M. M. Salary, H. Mosallaei, "Double split-loop resonators as building blocks of metasurfaces for light manipulation: Bending, focusing, and flat-top generation," *JOSA B*, vol. 33, no. 7, July 2016.
6. A. Forouzmand and H. Mosallaei, "All-dielectric C-shaped nanoantennas for light manipulation: Tailoring both magnetic and electric resonances to the desire," *Adv. Optical Mater.,* 1700147, DOI: 10.1002/adom.201700147.
7. A. Forouzmand and H. Mosallaei, "Shared aperture antenna for simultaneous two-dimensional beam steering at near-infrared and visible," *J. Nanophoton.* **11**(1), 010501 (2017).
8. A. Forouzmand, and H. Mosallaei, "Composite multilayer shared aperture nanostructures: A functional multispectral control," *ACS Photonics*, DOI: 10.1021/acsphotonics.7b01441, 2018.
9. S. Jafar-Zanjani, J. Cheng, V. Liberman, J. B. Chou, H. Mosallaei, "Large enhancement of third-order nonlinear effects with a resonant all-dielectric metasurface," *AIP Advances,* 6, 115213, 2016.
10. J. Cheng, S. Jafar-Zanjani, H. Mosallaei, "Real-Time Two-Dimensional Beam Steering with Gate-Tunable Materials: A Theory Design Investigation," *Applied Optics*, vol. 55, no. 22, 2016.
11. A. Forouzmand and H. Mosallaei, "Real-time controllable and multi-functional metasurfaces utilizing indium tin oxide materials: A phased array prospective," *IEEE Trans. Nanotechnology,* VOL. 16, NO. 2, pp. 296-306, March 2017.
12. A. Forouzmand, H. Mosallaei, "Tunable two dimensional optical beam steering with reconfigurable indium tin oxide plasmonic reflectarray metasurface," *Journal of Optics,* 18 (2016), 125003.
13. A. Forouzmand, M. M. Salary, S. Inampudi, and H. Mosallaei, "A tunable multigate indium-tin-oxide-assisted all-dielectric metasurface," *Adv. Optical Mater.,* 1701275, DOI: 10.1002/adom.201701275, 2018.
14. S. Jafar-Zanjani, J. Cheng, H. Mosallaei, "Light manipulation with flat and conformal inhomogeneous dispersive impedance sheets: An efficient FDTD modeling," *Applied Optics*, vol. 55, no. 11, 2016.
15. M. M. Salary and H. Mosallaei, "Electronically tunable metamaterials based on multimaterial nanowires incorporating transparent conductive oxides," *Scientific Report,* 7, 10055, DOI: 10.1038/s41598-017-09523-4, 2017.
16. M. M. Salary, A. Forouzmand, H. Mosallaei, "Controllable directive radiation from dipole emitter coupled to dielectric nanowire antenna with substrate-mediated tunability," *MRS Communications,* doi: 10.1557/mrc.2018.46.
17. M. M. Salary and H. Mosallaei, "Tunable magnetization of infrared epsilon-near-zero media via field-effect modulation," Applied Physics Letters **112**, 181104 (2018).
18. M. M. Salary, A. Forouzmand, and H. Mosallaei, "Model order reduction of large-scale metasurfaces using a hierarchical dipole approximation," *ACS Photonics,* DOI: 10.1021/acsphotonics.6b00568, 2016.
19. S. Tao, J. Cheng, H. Mosallaei, "An integral equation based domain decomposition method for solving large-size substrate-supported aperiodic plasmonic array platforms," *MRS Communications,* doi:10.1557/mrc.2016.11.

20. J. Cheng, S. Inampudi, and H. Mosallaei, "Optimization-based dielectric metasurfaces for angle-selective multifunctional beam deflection," *Scientific Report,* 7: 12228, DOI: 10.1038/s41598-017-12541-x, 2017.
21. S. Jafar-Zanjani, S. Inampudi, and H. Mosallaei, "Adaptive genetic algorithm for optical metasurfaces design," *Scientific Report,* 8:11040, DOI:10.1038/s41598-018-29275-z, 2018.

Changes in Research Objectives: None

Change in AFOSR Program Manager: None

Extension Granted or Milestones Slipped: Yes, extended till Sept 29, 2018

Include any New Discoveries, Inventions, or Patent Disclosures: None
Abstract: